



Spontaneous autophoretic motion of isotropic disks

Rodolfo Brandão¹ and Ehud Yariv^{1,†}

¹Department of Mechanical and Aerospace Engineering, Princeton University, Princeton, NJ 08544, USA

(Received 5 July 2023; revised 30 August 2023; accepted 3 September 2023)

It is theoretically known that an isotropic chemically active particle in an unbounded solution undergoes symmetry breaking when the intrinsic Péclet number Pe exceeds a finite critical value (Michelin *et al.*, *Phys. Fluids*, vol. 25, 2013, 061701). At that value, a transition takes place from a stationary state to spontaneous motion. In two dimensions, where no stationary state is possible in an unbounded domain, a linear stability analysis in a large bounded domain (Hu *et al.*, *Phys. Rev. Lett.*, vol. 123, 2019, 238004) reveals that the critical Pe value slowly diminishes as the domain size increases. Motivated by these findings, we here consider an unbounded domain from the outset, addressing the two-dimensional problem of steady self-propulsion with a focus on the limit $Pe \ll 1$. This singular limit is handled using matched asymptotic expansions, conceptually decomposing the fluid domain into a particle-scale region, where the leading-order solute transport is diffusive, and a remote region, where diffusion and advection are comparable. The expansion parameter is provided by the product of Pe and U , the unknown particle speed (normalised by the standard autophoretic scale). The problem is unconventional in that the scaling of U with Pe must be determined in the course of the perturbation analysis. The resulting approximation, $U = 4 \exp(-2/Pe - \gamma_E - 1)/Pe$ (γ_E being the Euler–Mascheroni constant), is in remarkable agreement with the numerical predictions of Hu *et al.* in the common interval of validity.

Key words: active matter, coupled diffusion and flow

1. Introduction

The prevailing continuum model of phoretic motion of chemically active particles in liquid solutions was introduced by Golestanian, Liverpool & Ajdari (2007). In that model, the

† On sabbatical leave. Permanent address: Department of Mathematics, Technion – Israel Institute of Technology, Haifa 32000, Israel. Email address for correspondence: yarivehud@gmail.com

solute undergoes diffusional transport. The chemical activity at the particle boundary is represented by a prescribed distribution of solute flux. The mechanical interaction of the solute with that boundary, in turn, is represented by diffusio-osmotic slip. Typically, fluid flow is animated by an imposed asymmetry in either the flux distribution or the particle shape. The particle instantaneously acquires the appropriate velocity so as to remain force- and torque-free.

Within that standard framework, a homogeneous isotropic particle in an unbounded liquid domain remains stationary, surrounded by a spherically symmetrical solute cloud. This situation changes dramatically when solute advection enters the picture (Jülicher & Prost 2009): introducing nonlinearity into the model, it may trigger a symmetry breaking. Indeed, Michelin, Lauga & Bartolo (2013) showed that when the intrinsic Péclet number Pe exceeds the critical value 4, the stationary state becomes unstable, resulting in spontaneous motion. The possibility of spontaneous motion in free solution has attracted significant attention in recent years (Saha, Yariv & Schnitzer 2021; Hu *et al.* 2022; Kailasham & Khair 2022; Peng & Schnitzer 2023; Schnitzer 2023), partly because of the linkage to active drops (Michelin 2023).

The prospect of spontaneous motion is particularly intriguing in two dimensions. With the Green's function of Laplace's equation varying as the logarithm of distance, a quiescent state in an unbounded domain is incompatible with the requirement for the solute concentration to approach an equilibrium value at large distances. In the absence of a stationary solution, it is impossible to detect spontaneous motion of an isotropic disk via a conventional stability analysis, as done in three dimensions. To circumvent this obstacle, Hu *et al.* (2019) introduced an artificial circular boundary of large radius (200 particle radii), centred about the particle. Since a stationary particle is an admissible solution for any Pe value in such a domain, Hu *et al.* (2019) were able to carry out a linear stability analysis, predicting a critical Péclet number (≈ 0.466 for that geometry) beyond which spontaneous motion emerges. The nonlinear problem governing that motion was solved numerically in that bounded domain. For yet larger Péclet numbers, Hu *et al.* (2019) found further transitions, first to meandering motion, then to circular motion and eventually to chaotic motion.

These two-dimensional (2-D) modes of spontaneous motion are theoretically attractive as they provide a simple set-up for complex phenomena. For example, Kailasham & Khair (2023) used a 2-D model to illustrate non-Brownian diffusion. It is therefore desirable to supplement the existing numerical simulations by analytic approximations. In pursuing that direction, it is natural to consider an unbounded configuration, as in the original three-dimensional (3-D) analysis of Michelin *et al.* (2013). This avoids the introduction of a superfluous parameter – the domain size. It should be emphasised that an artificial remote boundary is not required when analysing steady spontaneous motion: the advective–diffusive problem associated with that motion is expected to be well posed for any non-zero Pe (Sondak *et al.* 2016). That observation further suggests the consideration of the asymptotic limit $Pe \ll 1$, which provides a useful handle for a perturbation analysis. Since setting $Pe = 0$ reproduces the ill-posed problem, this is a singular limit.

We accordingly consider here steady spontaneous motion in an unbounded 2-D domain, focusing upon the limit $Pe \ll 1$. The problem of ‘conventional’ (non-spontaneous) steady 2-D autophoresis in that limit was handled in the literature (Yariv 2017; Yariv & Crowdy 2020; Saha & Yariv 2022) using singular perturbations, with separate asymptotic expansions in a particle-scale region and a remote Oseen-like region. The main difference between these asymptotic analyses and classical investigations of forced-convection problems (Acivos & Taylor 1962; Frankel & Acivos 1968) has to do with the

velocity field. In forced-convection problems, it is effectively prescribed; in autophoresis problems, it is driven by solute-concentration asymmetry. The need to solve for the flow and solute concentration simultaneously is essentially a technical difficulty, but it implies that the intrinsic Péclet number does not necessarily provide a true estimate of advective effects.

In the present context of spontaneous motion, that technical difficulty is amplified to a real challenge, since the flow is determined, not by any imposed asymmetry (absent for an isotropic particle), but rather by the need for an internal consistency of the asymptotic scheme. In particular, the very scaling with Pe of the particle velocity is unknown to begin with. This results in an unconventional asymptotic scheme where the dependence of the expansion parameter upon Pe is not known in advance; rather, it must be found throughout the analysis.

2. Problem formulation

We consider an idealised 2-D problem, with a circular particle (radius a^*) freely suspended in an unbounded liquid solution. The particle activity is modelled by a uniform solute flux j^* emanating from its boundary. The flow is driven by diffusio-osmosis, with the solution slipping along that boundary with a velocity provided by the product of the slip coefficient b^* (assumed uniform) and the surface gradient of the solute concentration. In addition to being passively advected by that flow, the solute diffuses in the liquid with a uniform diffusivity D^* . Following previous predictions of spontaneous motion (Michelin *et al.* 2013), we restrict the analysis to the relevant case where j^* and b^* have the same sign, so $b^*j^* > 0$.

Our interest is in the possibility of spontaneous motion, and in particular the steady-state speed U^* that the force-free particle acquires. Owing to the underlying isotropy, any direction is equally likely for the particle motion. We capture it using the unit vector $\hat{\mathbf{i}}$.

We employ a standard dimensionless notation, using a^* as a length scale, j^*a^*/D^* as a concentration scale and $U^* = b^*j^*/D^*$ as a velocity scale (Michelin *et al.* 2013). We formulate the problem in a particle-fixed reference frame, using polar coordinates (r, θ) with origin at the particle center and $\theta = 0$ in the upstream direction.

The excess concentration c , relative to the equilibrium concentration at large distances from the particle, is governed by: (i) the solute-transport equation,

$$\nabla^2 c = Pe \mathbf{u} \cdot \nabla c \quad \text{for } r > 1, \tag{2.1}$$

wherein

$$Pe = \frac{a^*U^*}{D^*} \tag{2.2}$$

is the intrinsic Péclet number; (ii) the imposed flux at the particle boundary,

$$\frac{\partial c}{\partial r} = -1 \quad \text{at } r = 1; \tag{2.3}$$

and (iii) the decay condition,

$$\lim_{r \rightarrow \infty} c = 0. \tag{2.4}$$

The velocity field \mathbf{u} is governed by: (i) the continuity and Stokes equations (the former tacitly employed in (2.1)); (ii) the slip condition,

$$\mathbf{u} = \nabla_s c \quad \text{at } r = 1; \tag{2.5}$$

(iii) the far-field approach to a uniform stream,

$$\lim_{r \rightarrow \infty} \mathbf{u} = -U\hat{\mathbf{i}}, \tag{2.6}$$

wherein $U = U^*/U^*$; and (iv) the requirement that the particle is force-free. The latter, in conjunction with (2.5) and (2.6), provides the particle velocity as a quadrature (Squires & Bazant 2006),

$$U = \frac{1}{2\pi} \int_{-\pi}^{\pi} \left. \frac{\partial c}{\partial \theta} \right|_{r=1} \sin \theta \, d\theta. \tag{2.7}$$

By the definition of $\hat{\mathbf{i}}$, U is positive. The nonlinearly coupled problem governing c and \mathbf{u} depends upon the single parameter Pe , which is strictly positive.

3. The limit $Pe \ll 1$

The underlying isotropy might appear to suggest a stationary state where c is radially symmetric, the velocity field vanishes and $U = 0$. Such a state, however, is incompatible with the decay condition (2.4): in two dimensions, the solution of Laplace’s equation with a finite flux diverges like $\ln r$ at large r . Fortunately, the nonlinear advective mechanism suggests the possibility of symmetry-broken solutions corresponding to spontaneous motion. With such motion, the advective term in (2.1) does not vanish. We claim that these solutions exist for arbitrarily small Pe values. To that end, we consider the asymptotic limit $Pe \ll 1$.

At this stage we do not know the scaling of U with Pe . In what follows, we proceed subject to an *a posteriori* verification that

$$Pe U \ll 1 \quad \text{for } Pe \ll 1. \tag{3.1}$$

Since \mathbf{u} is of order U (see (2.6)), it is evident from (2.1) that the relative magnitude of solute advection is $Pe U$, rather than Pe . (Note that $Pe U = a^*U^*/D^*$ represents the Péclet number associated with particle motion, cf. (2.2).) To reflect this estimate, we employ the rescaled velocity $\mathbf{v} = \mathbf{u}/U$. Thus, the advection–diffusion equation (2.1) becomes

$$\nabla^2 c = Pe U \mathbf{v} \cdot \nabla c \quad \text{for } r > 1; \tag{3.2}$$

the slip condition (2.5) reads

$$\mathbf{v} = U^{-1} \nabla_s c \quad \text{at } r = 1; \tag{3.3}$$

and the streaming condition (2.6) is simply

$$\lim_{r \rightarrow \infty} \mathbf{v} = -\hat{\mathbf{i}}. \tag{3.4}$$

With the latter being parameter-free, \mathbf{v} is expected to be $\text{ord}(1)$ in the limit $Pe \rightarrow 0$. Given (2.3), so is c .

With the pertinent small parameter in the problem being $Pe U$, we pose the generic asymptotic expansion,

$$f = f_0 + Pe U f_1 + \dots \quad (3.5)$$

We see from (3.2) that c_0 satisfies Laplace's equation,

$$\nabla^2 c_0 = 0. \quad (3.6)$$

The solution of (3.6) that satisfies (2.3) and is least singular at large r is the radially symmetric distribution,

$$c_0 = A_0 - \ln r. \quad (3.7)$$

That solution is incompatible with the decay requirement (2.4). To overcome this obstacle, we note that the (presumably subdominant) advective term in (3.2) becomes comparable to the diffusive term at distances of order $(Pe U)^{-1}$. Following this observation, we employ the method of matched asymptotic expansions (Hinch 1991). Thus, the fluid domain is conceptually decomposed into two asymptotic regions: a particle-scale region, $r = \text{ord}(1)$, where solute transport is dominated by diffusion; and a remote region, $r = \text{ord}(Pe^{-1}U^{-1})$, where the particle appears as point singularity. With that approach, the 'inner' expansion (3.5) is understood to hold at the particle region. The decay condition (2.4) does not apply in that region; rather, the concentration there is determined by the requirement of asymptotic matching with the comparable solution in the remote 'outer' region, which we address now.

4. Remote region

Defining the stretched coordinate,

$$r' = Pe U r, \quad (4.1)$$

the remote region is where $r' = \text{ord}(1)$. Writing $c(r, \theta) = c'(r', \theta)$, we find from (3.2) that the remote concentration c' is governed by

$$\nabla'^2 c' = \mathbf{v} \cdot \nabla' c', \quad (4.2)$$

wherein $\nabla' = (Pe U)^{-1} \nabla$ is the gradient operator in the stretched coordinates. In addition, it satisfies the decay condition (cf. (2.4))

$$\lim_{r' \rightarrow \infty} c' = 0. \quad (4.3)$$

Unlike the solute-transport problem, the flow problem does not exhibit any form of non-uniformity. Indeed, with a force-free condition, the Stokes equations hold throughout. In fact, as the flow is coupled to the solute concentration only through the slip condition (3.3), no need arises for a comparable rescaling of the flow variables in the remote region. Rather, the flow there is simply extracted by replacing r with $(Pe U)^{-1} r'$ and expanding for small $Pe U$. In particular, it follows from (3.4) that, for r' fixed, \mathbf{v} possesses the asymptotic expansion

$$\mathbf{v} \sim -\hat{\mathbf{i}} + \dots \quad (4.4)$$

Thus, the leading-order flow is uniform in the remote region.

Given the above observation, the only asymptotic expansion required in the remote region is that of the concentration. Employing an expansion akin to (3.5), we only seek the leading-order concentration c'_0 . Substituting (4.4) into (4.2) we obtain

$$\nabla'^2 c'_0 = -\frac{\partial c'_0}{\partial x'}, \tag{4.5}$$

where $x' = r' \cos \theta$ is a stretched Cartesian coordinate in the direction of \hat{i} . The solution of (4.5) that satisfies (4.3) and is least singular at the origin is (Wilson 1904)

$$c'_0 = \frac{Q}{2\pi} K_0(r'/2) \exp(-x'/2), \tag{4.6}$$

in which K_0 is the modified Bessel function of the second kind. The source magnitude Q , appearing in (4.6), remains to be determined.

Using the small-argument behaviour of K_0 (Abramowitz & Stegun 1965), we find

$$c'_0 \sim -\frac{Q}{2\pi} \left(\ln \frac{r'}{4} + \gamma_E \right) \quad \text{as } r' \rightarrow 0, \tag{4.7}$$

wherein $\gamma_E = 0.57721 \dots$ is the Euler–Mascheroni constant. The asymptotic error in (4.7) is ‘algebraically small’ in r' , i.e. smaller than some positive power of r' . Thus, application of ord(1) : ord(1) Van Dyke matching gives

$$c_0 \sim -\frac{Q}{2\pi} \left(\ln \frac{Pe Ur}{4} + \gamma_E \right) \quad \text{as } r \rightarrow \infty. \tag{4.8}$$

Comparison with (3.7) gives $Q = 2\pi$ and

$$A_0 = \ln \frac{4}{Pe U} - \gamma_E. \tag{4.9}$$

In our analysis we allow for the respective coefficients in both (3.5) and the comparable outer expansion to depend weakly upon the expansion parameter through its logarithm (as in (4.9)). This practice enables the use of the Van Dyke matching rule (Van Dyke 1964) subject to Fraenkel’s principle (Fraenkel 1969), according to which distinct asymptotic orders are separated only by the powers of the expansion parameter, while asymptotic terms that differ by its logarithm are grouped together.

5. Beyond radial symmetry

The radially symmetric distribution (3.7) does not result in fluid motion; see (3.3) (or, equivalently, (2.7)). We therefore need to consider the next term in the inner expansion, c_1 . Its asymmetry is driven by higher-order matching with the remote concentration. Indeed, expanding (4.6) at small r' up to ord(r') yields the following refinement of (4.7),

$$c'_0 \sim -\left(\ln \frac{r'}{4} + \gamma_E \right) \left(1 - \frac{1}{2} r' \cos \theta \right) \quad \text{as } r' \rightarrow 0, \tag{5.1}$$

where the relative asymptotic error is algebraically small compared to r' .

Thus, the leading-order correction c_1 satisfies the far-field condition,

$$c_1 \sim \frac{1}{2} \left(\ln \frac{Pe Ur}{4} + \gamma_E \right) r \cos \theta \quad \text{as } r \rightarrow \infty, \quad (5.2)$$

which follows from Van Dyke ord(1) : ord($Pe U$) matching. In addition, it is governed by the differential equation (see (3.2))

$$\nabla^2 c_1 = -\frac{\mathbf{v}_0 \cdot \hat{\mathbf{e}}_r}{r} \quad \text{for } r > 1, \quad (5.3)$$

and the no-flux condition (see (2.3))

$$\frac{\partial c_1}{\partial r} = 0 \quad \text{at } r = 1. \quad (5.4)$$

Equation (5.3) couples c_1 to the leading-order velocity field \mathbf{v}_0 . That field, in turn, is governed by the continuity and Stokes equations together with the slip condition (recall (3.3)),

$$\mathbf{v}_0 = Pe \nabla_s c_1 \quad \text{at } r = 1. \quad (5.5)$$

Given the absence of scale separation in the flow problem, \mathbf{v}_0 is subject to the streaming condition (cf. (3.4))

$$\lim_{r \rightarrow \infty} \mathbf{v}_0 = -\hat{\mathbf{i}}. \quad (5.6)$$

Last, \mathbf{v}_0 must be compatible with the force-free condition at leading order. The latter is equivalent to the requirement (cf. (2.7))

$$Pe \int_{-\pi}^{\pi} \frac{\partial c_1}{\partial \theta} \Big|_{r=1} \sin \theta \, d\theta = 2\pi, \quad (5.7)$$

or, following integration by parts,

$$Pe \int_{-\pi}^{\pi} c_1|_{r=1} \cos \theta \, d\theta = -2\pi. \quad (5.8)$$

6. An apparent contradiction and its resolution

With $Pe \ll 1$, (5.5) may appear to imply that \mathbf{v}_0 actually satisfies a no-slip condition. Such a condition, however, is incompatible with (5.6): there is no solution to the Stokes equations in two dimensions that satisfies both conditions – this is the well-known Stokes paradox (Leal 2007). A related apparent contradiction is evident from (5.8), which seems incompatible with the underlying limit $Pe \ll 1$.

These incompatibilities may be traced back to the original problem. With c_0 given by (3.7), it is clear from (3.5) that the deviation of c from a radially symmetric distribution is of order $Pe U$. Then, the slip condition (2.5) (or, equivalently, the force-free constraint (2.7)) suggests that U is of the same order. It may therefore appear that Pe must be ord(1), contradicting our starting point $Pe \ll 1$. Of course, when Pe is of order unity there is no perturbation parameter in the problem, so the entire asymptotic analysis becomes meaningless.

The resolution of these apparent conflicts has to do with the interpretation of logarithmically small terms when adhering to the asymptotic practice of separating by powers of the expansion parameter. Thus, if it turns out that Pe is ‘logarithmically small’

with respect to the expansion parameter $Pe U$, no contradiction arises. To see that this is indeed the case, we note that (5.2) suggests that c_1 is of order $\ln(Pe U)$, while (5.5) necessitates it to be $1/Pe$. Balancing these terms, we conclude that

$$Pe U = \text{ord}(e^{-\text{const.}/Pe}), \tag{6.1}$$

wherein the positive constant is as yet unknown. Thus, $1/Pe$ is indeed of the order of the logarithm of the small expansion parameter $Pe U$. Incidentally, (6.1) provides an *a posteriori* justification for (3.1).

The scaling (6.1) suggests the following expansion,

$$U = \frac{\exp(-k(Pe)/Pe)}{Pe} + \dots, \tag{6.2}$$

where the function $k(Pe)$, which remains to be determined, has a non-zero limit as $Pe \rightarrow 0$.

We anticipate that the asymptotic error in (6.2) is exponentially small in Pe . The asymptotic behaviour (5.2) now reads

$$c_1 \sim \frac{1}{2} \left(\ln \frac{r}{4} - \frac{k}{Pe} + \gamma_E \right) r \cos \theta \quad \text{as } r \rightarrow \infty. \tag{6.3}$$

7. Irrotational-flow solution

At this stage we need to solve two mutually coupled linear problems: the asymmetric concentration problem, governed by (5.3), (5.4) and (6.3); and the flow problem, governed by the continuity and Stokes equations together with (5.5), (5.6) and the force-free condition, equivalent to (5.8). We emphasise that Pe , which appears in these problems, is now interpreted as a logarithmically small term. We do not (and should not) make use of its smallness in solving these problems.

Given the no-flux condition (5.4), the surface-gradient operator in the slip condition (5.5) may be replaced by the standard gradient operator, giving

$$v_0 = Pe \nabla c_1 \quad \text{at } r = 1. \tag{7.1}$$

Following classical treatments in phoretic motion (Morrison 1970), it is then tempting to seek an irrotational flow, of the form $Pe \nabla c_1$, which would trivially satisfy the above slip condition, as well as the Stokes equations and force-free constraint. However, such a form would violate the continuity equation, since c_1 is not harmonic – see (5.3).

It turns out that the irrotational *ansatz* is nonetheless instrumental in constructing the solution, but some care is needed. Thus, we postulate

$$v_0 = \nabla \varphi, \tag{7.2}$$

where the velocity potential φ is defined to within an arbitrary additive constant, which is physically irrelevant. The continuity equation implies that φ is harmonic,

$$\nabla^2 \varphi = 0 \quad \text{for } r > 1. \tag{7.3}$$

The Stokes equations are then trivially satisfied (with nil pressure), as is the force-free condition. The slip condition (5.5) implies that φ satisfies the homogeneous Neumann

condition,

$$\frac{\partial \varphi}{\partial r} = 0 \quad \text{at } r = 1, \tag{7.4}$$

while the far-field streaming (5.6) implies that

$$\varphi \sim -r \cos \theta \quad \text{as } r \rightarrow \infty. \tag{7.5}$$

The solution of (7.3)–(7.5) is simply

$$\varphi = -\left(r + \frac{1}{r}\right) \cos \theta. \tag{7.6}$$

The associated velocity field (7.2) is

$$\mathbf{v}_0 = -\hat{\mathbf{e}}_r(1 - r^{-2}) \cos \theta + \hat{\mathbf{e}}_\theta(1 + r^{-2}) \sin \theta. \tag{7.7}$$

Inspired by (7.1), we write

$$c_1 = Pe^{-1}\varphi + \chi, \tag{7.8}$$

where

$$\chi = \text{const.} \quad \text{at } r = 1, \tag{7.9}$$

so that (7.2) guarantees the satisfaction of the slip condition (5.5). In what follows, we seek the ‘adjustment’ χ . From (5.3), (7.3) and (7.7) we see that it is governed by the Poisson equation,

$$\nabla^2 \chi = (r^{-1} - r^{-3}) \cos \theta \quad \text{for } r > 1. \tag{7.10}$$

From (5.4) and (7.4) we further observe that it satisfies a homogeneous Neumann condition at $r = 1$. The solution of the above problem that satisfies (7.9) is

$$\chi = \frac{1}{2} \left(r \ln r - r + \frac{\ln r}{r} + \frac{1}{r} \right) \cos \theta + \text{const.} \tag{7.11}$$

Given (7.6) and (7.9), constraint (5.8) is trivially satisfied. This was to be expected, as that constraint follows from the combination of the slip and force-free conditions; these have already been enforced.

Comparing (7.6), (7.8) and (7.11) with the dictated asymptotic behaviour (6.3), we observe that the terms proportional to $r \ln r$ trivially match, while agreement of the terms proportional to r itself necessitates

$$k = 2 + Pe(1 + \gamma_E - \ln 4). \tag{7.12}$$

This completes the analysis at $\text{ord}(Pe U)$. In principle, the constant appearing in (7.11) may be obtained using higher-order asymptotic matching. Its value, however, is immaterial to our goal – the calculation of U .

8. Phoretic speed

Plugging (7.12) into (6.2) yields the requisite approximation

$$U = \frac{4 \exp(-2/Pe - \gamma_E - 1)}{Pe}. \tag{8.1}$$

The constant in (6.1) is 2. The remote scale $(Pe U)^{-1}$ is of order $\exp(2/Pe)$.

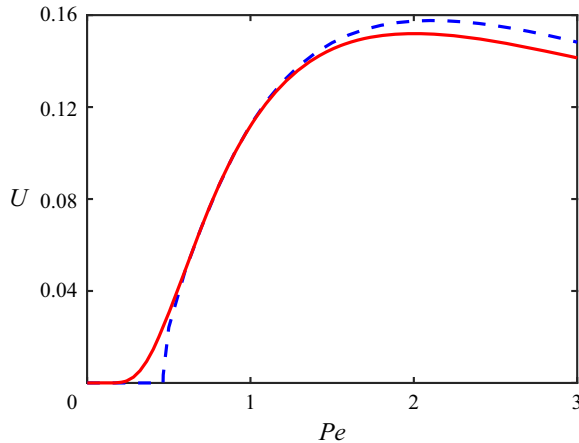


Figure 1. Spontaneous speed as a function of Pe . The solid curve is the present (8.1). The dashed curve represents the straight-motion speed displayed in figure 1 of Hu *et al.* (2019).

We can now understand the prediction of a critical Pe by Hu *et al.* (2019), who introduced an artificial boundary at $r = R$. For the remote transport at distances $\exp(2/Pe)$ to be captured in a finite region $r < R$, one roughly needs $Pe \gtrsim 2/\ln R$. For smaller Pe , no spontaneous motion can be predicted. For a given R , the associated critical Pe merely indicates the transition to a geometry where the bounded problem indeed emulates the unbounded one. It is interesting to note that Hu *et al.* (2019) derived the same estimate for the critical Pe using their stability analysis in the finite-domain problem.

In figure 1 we compare the present (8.1) with the spontaneous speed predicted by Hu *et al.* (2019), who took $R = 200$. For that value, $2/\ln R$ is roughly 0.4. The critical Péclet number found by Hu *et al.* (2019), ≈ 0.466 , is indeed close to that value. For larger Pe , we observe in figure 1 an interval where the present (8.1) and the prediction of Hu *et al.* (2019) are virtually indistinguishable. (While the present approximation is strictly valid for $Pe \ll 1$, it is remarkably accurate up to about $Pe = 1$.) When Pe is larger still, the small- Pe approximation (8.1) becomes irrelevant, and the two predictions separate off.

9. Concluding remarks

Given the absence of a reference stationary state, the concept of a critical Pe in 2-D unbounded domains becomes vague. This is corroborated by the numerical predictions (Hu *et al.* 2019) of a critical Péclet number that diminishes slowly to zero as the distance to the remote boundary is enlarged. The prediction of a critical Péclet number, based upon a linear stability analysis, is accordingly irrelevant for the unbounded problem. Moreover, the nonlinear advection–diffusion problem governing spontaneous motion is expected to be well posed in the unbounded configuration for any finite Pe .

We therefore advocate for the use of unbounded domains in theoretical investigations of 2-D spontaneous motion, mimicking the idealised configurations studied in three dimensions. Adopting this conceptual approach, we have addressed herein the unbounded problem from the outset. Our work reveals that spontaneous motion occurs for arbitrarily small Péclet numbers. This is fundamentally different from the 3-D case (Michelin *et al.* 2013).

The present analysis may be extended to incorporate more realistic descriptions of interfacial activity, where the prescribed flux is replaced by a first-order kinetic model

(Ebbens *et al.* 2012; Li 2022). Since that model still gives rise to a logarithmic divergence with distance in a 2-D diffusive transport (Yariv 2017; Yariv & Crowdy 2020; Saha & Yariv 2022), the stationary state remains ill posed. It is therefore anticipated that, even with a more realistic interfacial description, spontaneous motion emerges at arbitrarily small Péclet numbers.

Funding. E.Y. was supported by the United States–Israel Binational Science Foundation (Grant No. 2019642).

Declaration of interests. The authors report no conflict of interest.

Author ORCIDs.

 Rodolfo Brandão <https://orcid.org/0000-0002-1544-1162>;

 Ehud Yariv <https://orcid.org/0000-0003-0398-2954>.

REFERENCES

- ABRAMOWITZ, M. & STEGUN, I.A. 1965 *Handbook of Mathematical Functions*, 3rd edn. Dover.
- ACRIVOS, A. & TAYLOR, T.D. 1962 Heat and mass transfer from single spheres in Stokes flow. *Phys. Fluids* **5** (4), 387–394.
- EBBENS, S., TU, M.-H., HOWSE, J.R. & GOLESTANIAN, R. 2012 Size dependence of the propulsion velocity for catalytic Janus-sphere swimmers. *Phys. Rev. E* **85** (2), 020401.
- FRAENKEL, L.E. 1969 On the methods of matched asymptotic expansions. Part 1. A matching principle. *Proc. Camb. Phil. Soc.* **65**, 209–231.
- FRANKEL, N.A. & ACRIVOS, A. 1968 Heat and mass transfer from small spheres and cylinders freely suspended in shear flow. *Phys. Fluids* **11**, 1913–1918.
- GOLESTANIAN, R., LIVERPOOL, T.B. & AJDARI, A. 2007 Designing phoretic micro- and nano-swimmers. *New J. Phys.* **9**, 126.
- HINCH, E.J. 1991 *Perturbation Methods*. Cambridge University Press.
- HU, W.-F., LIN, T.-S., RAFAI, S. & MISBAH, C. 2019 Chaotic swimming of phoretic particles. *Phys. Rev. Lett.* **123** (23), 238004.
- HU, W.-F., LIN, T.-S., RAFAI, S. & MISBAH, C. 2022 Spontaneous locomotion of phoretic particles in three dimensions. *Phys. Rev. Fluids* **7** (3), 034003.
- JÜLICHER, F. & PROST, J. 2009 Generic theory of colloidal transport. *Eur. Phys. J. E* **29** (1), 27–36.
- KAILASHAM, R. & KHAIR, A.S. 2022 Dynamics of forced and unforced autophoretic particles. *J. Fluid Mech.* **948**, A41.
- KAILASHAM, R. & KHAIR, A.S. 2023 Non-Brownian diffusion and chaotic rheology of autophoretic disks. *Phys. Rev. E* **107** (4), 044609.
- LEAL, L.G. 2007 *Advanced Transport Phenomena: Fluid Mechanics and Convective Transport Processes*. Cambridge University Press.
- LI, G. 2022 Swimming dynamics of a self-propelled droplet. *J. Fluid Mech.* **934**, A20.
- MICHELIN, S. 2023 Self-propulsion of chemically active droplets. *Annu. Rev. Fluid Mech.* **55**, 77–101.
- MICHELIN, S., LAUGA, E. & BARTOLO, D. 2013 Spontaneous autophoretic motion of isotropic particles. *Phys. Fluids* **25** (6), 061701.
- MORRISON, F.A. 1970 Electrophoresis of a particle of arbitrary shape. *J. Colloid Interface Sci.* **34**, 210–214.
- PENG, G.G. & SCHNITZER, O. 2023 Weakly nonlinear dynamics of a chemically active particle near the threshold for spontaneous motion. II. History-dependent motion. *Phys. Rev. Fluids* **8** (3), 033602.
- SAHA, S. & YARIV, E. 2022 Phoretic self-propulsion of a slightly inhomogeneous disc. *J. Fluid Mech.* **940**, A24.
- SAHA, S., YARIV, E. & SCHNITZER, O. 2021 Isotropically active colloids under uniform force fields: from forced to spontaneous motion. *J. Fluid Mech.* **916**, A47.
- SCHNITZER, O. 2023 Weakly nonlinear dynamics of a chemically active particle near the threshold for spontaneous motion. I. Adjoint method. *Phys. Rev. Fluids* **8** (3), 034201.
- SONDAK, D., HAWLEY, C., HENG, S., VINSONHALER, R., LAUGA, E. & THIFFEAULT, J.-L. 2016 Can phoretic particles swim in two dimensions? *Phys. Rev. E* **94** (6), 062606.
- SQUIRES, T.M. & BAZANT, M.Z. 2006 Breaking symmetries in induced-charge electro-osmosis and electrophoresis. *J. Fluid Mech.* **560**, 65–101.
- VAN DYKE, M. 1964 *Perturbation Methods in Fluid Mechanics*. Academic Press.

- WILSON, H.A. 1904 On convection of heat. *Proc. Camb. Phil. Soc.* **12** (5), 406–423.
- YARIV, E. 2017 Two-dimensional phoretic swimmers: the singular weak-advection limits. *J. Fluid Mech.* **816**, R3.
- YARIV, E. & CROWDY, D. 2020 Phoretic self-propulsion of Janus disks in the fast-reaction limit. *Phys. Rev. Fluids* **5** (11), 112001(R).